

Synthesis, and characterization of new Cd^{2+} , Hg^{2+} complexes of thiosemicarbazone ligand derived from beta hydroxy carbonyl.

Ibrahim A. Abdelwahed^a, Gaber M. Abu El-Reash^{a,*}, Magdy M. Youssef^a

^a Chemistry Department, Faculty of Science, Mansoura University, Mansoura, 35516, Egypt.

* Correspondence to: gaelreash@mans.edu.eg, 01000373155)

Received: 15/10/2023
Accepted: 25/11/2023

Abstract In this work, new Cd^{2+} , and Hg^{2+} complexes of 4-pyridyl thiosemicarbazone Schiff base derived from beta-hydroxy carbonyl has been synthesized and isolated. The structure of the new complexes was proposed by numerous techniques such as elemental (CHN) analyses, FT-IR. TG and DTG thermal decomposition for Cd^{2+} complex was carried out. Thermodynamic and kinetic parameters were calculated via Coats-Redfern and Horowitz-Metzger equations. And finally, the modeling using DFT calculations was fully studied.

keywords: 4-pyridyl thiosemicarbazone, DFT, beta-hydroxy carbonyl.

1. Introduction

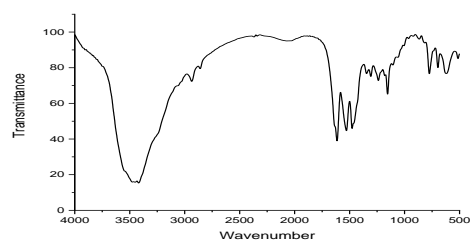
Thiosemicarbazone compounds and their derivatives attracted a lot of interest from chemists and biologists due to their highly stable colored chelates with a wide diversity of stereochemistry for the spectrophotometric detection of metal ions in various environments [1]. In addition, to their antiviral [2] antibacterial [3] and anticancer [4] properties. The presence of the imine ($-\text{C}=\text{N}-$) group in the semicarbazone and thiosemicarbazone frameworks was essential for the compounds' antibacterial action mechanism [5]. Thiosemicarbazones are notable for their considerable pharmacological characteristics as well as an intriguing and adaptable manner of chelation in their complexes [6, 7]. Due of their biological characteristics, pyridine-ringed thiosemicarbazones and related metal derivatives have undergone substantial research [8]. Additionally, the thiosemicarbazones with heterocyclic rings can form a tridentate XNS complexes ($\text{X} = \text{O}, \text{N}, \text{S}$) with a metal ion [9]. In this work we will study new Cd^{2+} in form of $[\text{Cd}(\text{H}_2\text{L})\text{Cl}(\text{H}_2\text{O}) \cdot 2\text{H}_2\text{O}$ (1), and Hg^{2+} in form of $[\text{Hg}(\text{HL})\text{H}_2\text{O}]$ (2) thiosemicarbazone metal complexes.

2. Results and Discussion

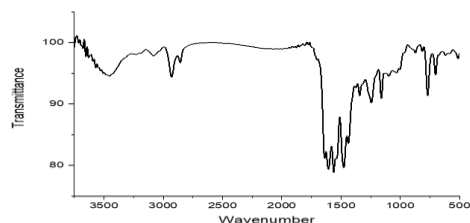
2.1. FT-IR spectra interpretation

In Cd^{2+} complex (1) IR spectrum (Figure 1), ligand behaved as monobasic bidentate manner in binding with metal ion through N atom in

($\text{C}=\text{N}$) azomethine, and S atom in thione form ($\text{C}=\text{S}$) group, this binding behavior can be supported by the strongly observed shifts in $\nu(\text{C}=\text{N})$ azomethine, and $\nu(\text{C}=\text{S})$ bands. In Hg^{2+} complex (2) IR spectrum (Figure 2), ligand binds with metal ion via dibasic tridentate manner by N atom in ($\text{C}=\text{N}$) azomethine, S atom in thione form ($\text{C}=\text{S}$) group, and O atom in ($-\text{OH}$) group, which is strongly indicated by the highly observable shifts in $\nu(\text{C}=\text{N})$ azomethine, $\nu(\text{C}=\text{S})$ bands, and significant quenching in $\nu(\text{OH})$ band compared to that in ligand.



(1)



(2)

Figure 1: FT-IR Spectrum of (1), and (2) Complexes

2.2. Thermogravimetric & Kinetic Data Analysis

Cd^{2+} complex decomposed in three main steps as illustrated in Figure 2, plus one final step for residue, (Kinetic data showing in Table 1, and Figures 3, 4) the steps took the following track, first step was at temperature range 38.60-371.48 °C included the loss of 3 H_2O molecules in form of 2 hydrated molecules, and 1 coordinated molecule, plus the loss of N_4H_8 fragment in weight loss = % Found (Calculated) 21.65 (21.27). The second step was at temperature range 371.48-658.71 °C included the loss of $\text{C}_2\text{H}_4\text{O}_2$ fragment in weight loss = 11.07 (10.89). Third step took place at temperature range 658.71-867.81 °C included loss of $\text{C}_{17}\text{H}_{11}\text{S}$ fragment with weight loss = 44.57 (44.72). The final step was for the residue. Included loss of CdO in weight loss = 23.23 (23.12) at temperature range of 867.81-1000 °C.

2.3 Molecular Modeling

2.3.1 Geometry Optimization

For complex Cd^{2+} (1), In Figure 5, and bonds lengths data recorded in Table 2, we observe a change in bonds N(10)-C(11), N(10)-N(9), and S(17)-C(8) in H_3L ligand from 1.263, 1.352, and 1.576 to 1.274, 1.253, and 1.506 Å respectively in complex as a result of participation of atoms N(10), and S(17) in bonding with Cd^{2+} ion.

In complex Hg^{2+} (2) model Figure 6, and bonds lengths data recorded in Table 3, we observe a change in bonds N(10)-N(9), N(10)-C(11), S(17)-C(8), O(25)-C(18) in H_3L from 1.352, 1.263, 1.579, and 1.418 to 1.333, 1.271, 1.715, and 1.435 Å in complex as a result of participation of atoms N(10), S(17), and O(25) in bonding with Hg^{2+} ion

Table 1: Kinetic Parameters of complex $[\text{Cd}(\text{H}_2\text{L}^2)\text{Cl}(\text{H}_2\text{O})\cdot 2\text{H}_2\text{O}$ Evaluated by Horowitz-Metzger, and Coats-Redfern Equations.

Step	Mid Temp (K)	Method	order (n)	R^2	E_a KJ/mol	A (S^{-1})	ΔH^* KJ/mol	ΔS^* KJ/mol.K	ΔG^* KJ/mol
1 st	517.78	HM	1.00	0.95	76.18	150472.95	71.88	-0.15	149.74
		CR	1.00	0.96	66.57	17631.12	62.27	-0.16	149.36
2 nd	734.06	HM	1.00	0.97	291.17	1.88×10^{18}	285.06	0.097	213.53
		CR	1.00	0.97	285.90	8.29×10^{17}	279.80	0.090	213.27
3 rd	1078.44	HM	1.00	0.97	352.30	3.34×10^{14}	343.33	0.022	319.10
		CR	1.00	0.97	336.64	6.10×10^{13}	327.67	0.008	318.71

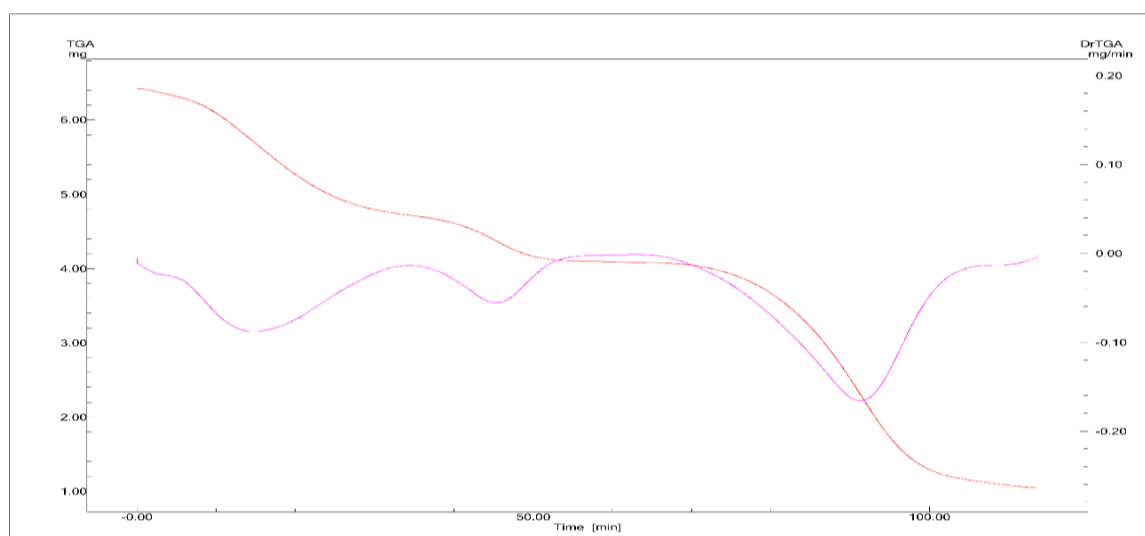


Figure 2: Thermal Decomposition Steps for Cd^{2+} Complex

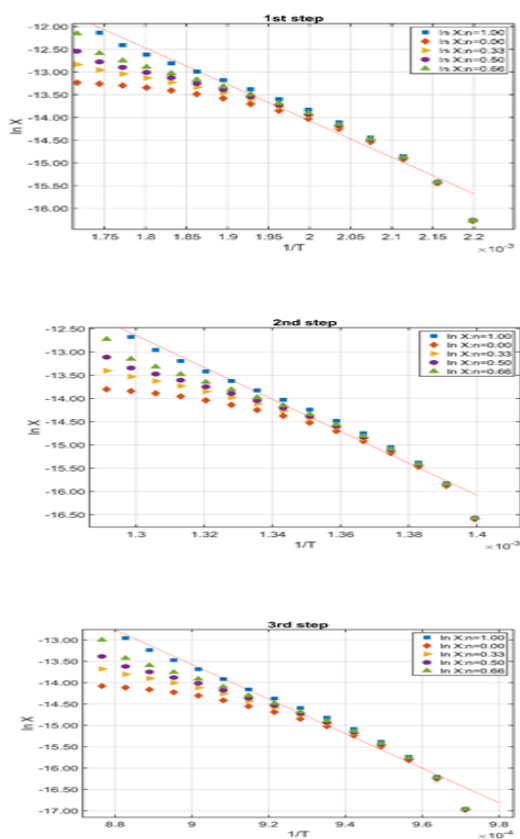


Figure 3: Coats-Redfern Steps for Cd²⁺ Complex

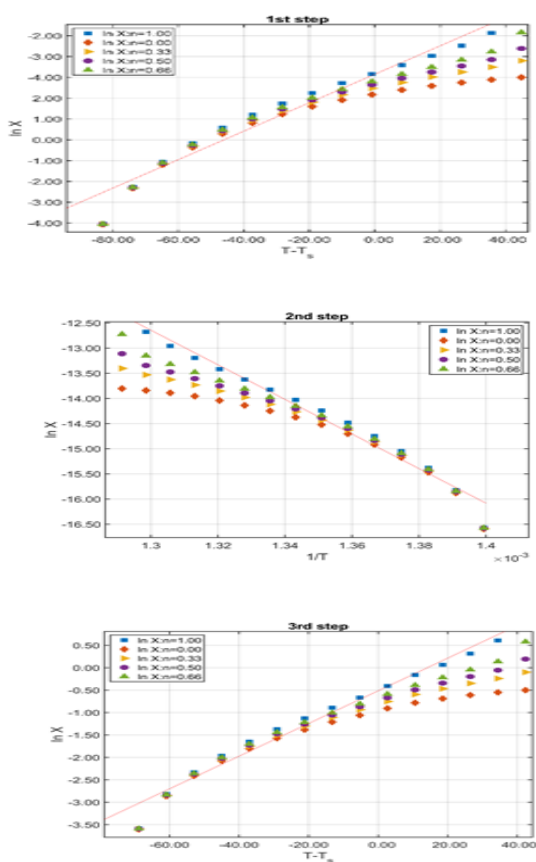


Figure 4: Horowitz-Metzger Steps for Cd²⁺ Complex

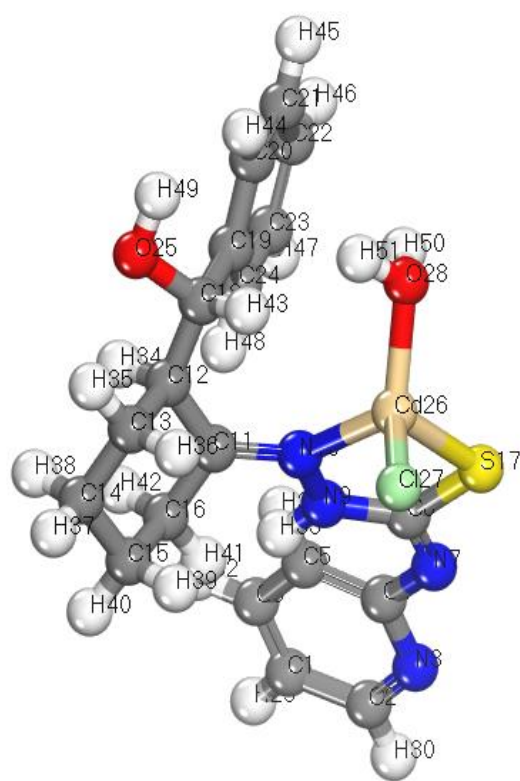


Figure 5: 3D Structure of Cd²⁺ Complex with Atom Numbering

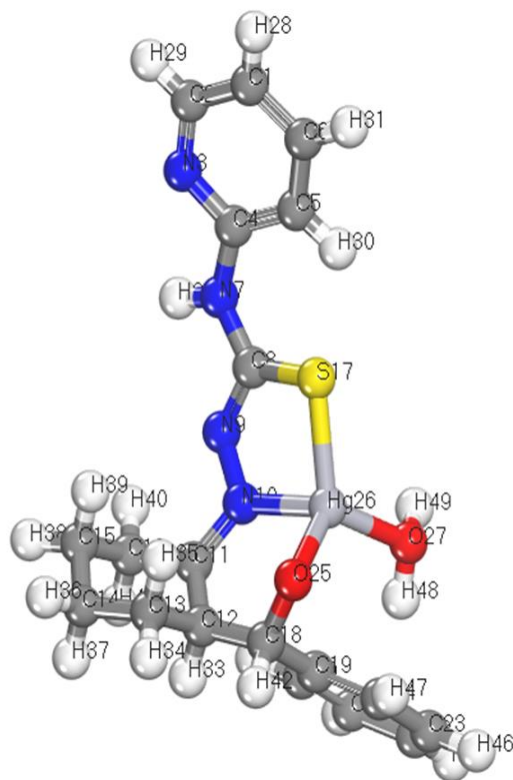


Figure 6: 3D Structure of Hg²⁺ Complex (2) with Atom Numbering

Table 2: Bond Lengths of Complex Cd²⁺

Bond	Length (Å)	Bond	Length (Å)	Bond	Length (Å)
O(28)-H(51)	0.992	N(9)-H(33)	1.052	N(10)-Cd(26)	2.168
O(28)-H(50)	1.025	C(6)-H(32)	1.103	S(17)-Cd(26)	2.508
O(25)-H(49)	0.961	C(5)-H(31)	1.099	Cd(26)-Cl(27)	2.474
C(24)-H(48)	1.1	C(2)-H(30)	1.103	C(18)-O(25)	1.42
C(23)-H(47)	1.103	C(1)-H(29)	1.102	C(18)-C(19)	1.521
C(22)-H(46)	1.103	C(19)-C(24)	1.346	C(12)-C(18)	1.531
C(21)-H(45)	1.103	C(23)-C(24)	1.342	C(8)-S(17)	1.506
C(20)-H(44)	1.103	C(22)-C(23)	1.341	C(16)-C(11)	1.52
C(18)-H(43)	1.108	C(21)-C(22)	1.341	C(15)-C(16)	1.537
C(16)-H(42)	1.114	C(20)-C(21)	1.342	C(14)-C(15)	1.537
C(16)-H(41)	1.116	C(19)-C(20)	1.347	C(13)-C(14)	1.541
C(15)-H(40)	1.116	C(5)-C(4)	1.35	C(12)-C(13)	1.544
C(15)-H(39)	1.117	N(3)-C(4)	1.274	C(11)-C(12)	1.521
C(14)-H(38)	1.117	C(2)-N(3)	1.265	N(10)-C(11)	1.274
C(14)-H(37)	1.116	C(1)-C(2)	1.34	N(9)-N(10)	1.253
C(13)-H(36)	1.112	C(6)-C(1)	1.339	C(8)-N(9)	1.284
C(13)-H(35)	1.115	C(5)-C(6)	1.342	N(7)-C(8)	1.274
C(12)-H(34)	1.121	O(28)-Cd(26)	2.151	C(4)-N(7)	1.272

Table 3: Bond Lengths of Hg²⁺ Complex (2)

Bond	Length (Å)	Bond	Length (Å)	Bond	Length (Å)
O(27)-H(49)	1.004	C(6)-H(31)	1.103	O(25)-Hg(26)	2.197
O(27)-H(48)	1.021	C(5)-H(30)	1.096	S(17)-Hg(26)	2.536
C(24)-H(47)	1.103	C(2)-H(29)	1.103	C(18)-O(25)	1.435
C(23)-H(46)	1.103	C(1)-H(28)	1.101	C(18)-C(19)	1.54
C(22)-H(45)	1.103	C(19)-C(24)	1.348	C(12)-C(18)	1.582
C(21)-H(44)	1.103	C(23)-C(24)	1.341	C(8)-S(17)	1.715
C(20)-H(43)	1.1	C(22)-C(23)	1.34	C(16)-C(11)	1.507
C(18)-H(42)	1.121	C(21)-C(22)	1.34	C(15)-C(16)	1.538
C(16)-H(41)	1.114	C(20)-C(21)	1.342	C(14)-C(15)	1.54
C(16)-H(40)	1.115	C(19)-C(20)	1.347	C(13)-C(14)	1.542
C(15)-H(39)	1.117	C(5)-C(4)	1.35	C(12)-C(13)	1.541
C(15)-H(38)	1.116	N(3)-C(4)	1.275	C(11)-C(12)	1.553
C(14)-H(37)	1.117	C(2)-N(3)	1.264	N(10)-C(11)	1.271
C(14)-H(36)	1.117	C(1)-C(2)	1.339	N(9)-N(10)	1.333
C(13)-H(35)	1.115	C(6)-C(1)	1.338	C(8)-N(9)	1.374
C(13)-H(34)	1.116	C(5)-C(6)	1.343	N(7)-C(8)	1.284
C(12)-H(33)	1.123	N(10)-Hg(26)	2.181	C(4)-N(7)	1.279
N(7)-H(32)	1.056	O(27)-Hg(26)	2.241		

3.2 Molecular Frontier & MESP

Table 4: E_{HOMO}, and E_{LUMO} for Cd²⁺ complex.

Compound	E _H (eV)	E _L (eV)	ΔE (E _H -E _L) (eV)	X (eV)	μ (eV)	η (eV)	S (eV ⁻¹)	ω (eV)	σ (eV)	ΔN _{max}
Cd ²⁺ (1)	-3.667	-1.950	1.717	2.809	-2.809	0.859	0.429	4.594	1.165	3.271
Hg ²⁺ (2)	-4.615	-1.922	2.693	3.269	-3.269	1.347	0.673	3.967	0.743	2.427

Energy Band Gap (E_H - E_L) Electronegativity (X) Chemical Potential (μ) Reactivity Index (ΔN_{max})
Hardness (η) Softness (S) Global Electrophilicity Index (ω) Global Hardness (σ)

HOMO-LUMO (molecular orbitals at the frontier) analysis (Figure 7) is an essential data to assess the compound's chemical reactivity. The electron donor orbital known as the HOMO identifies electrophiles, while LUMO acts as an electron acceptor orbital and identifies nucleophiles; The data recorded in Table 4 describes the energy gap $\Delta E = (E_H - E_L)$ and local reactivity descriptors such as η and S values are used to anticipate the molecule's reactivity and stability, while X is a measure of an atom's capacity to draw shared electrons to itself. μ values gauges the electrons' capacity to

break free of their equilibrium framework, ω assesses a molecule's capacity to accept electrons [10, 11].

3D graphs (MESP maps) for Cd^{2+} , and Hg^{2+} complexes are shown in Figure 8. The largest positive portion is the preferred location to nucleophilic attack, is shown in blue. While the largest negative portion, which is the favored site for electrophilic attack, is displayed in red. As the potential drops from blue to green to red, blue shows the most chosen attraction site, while red indicates the most desired site for repulsion.

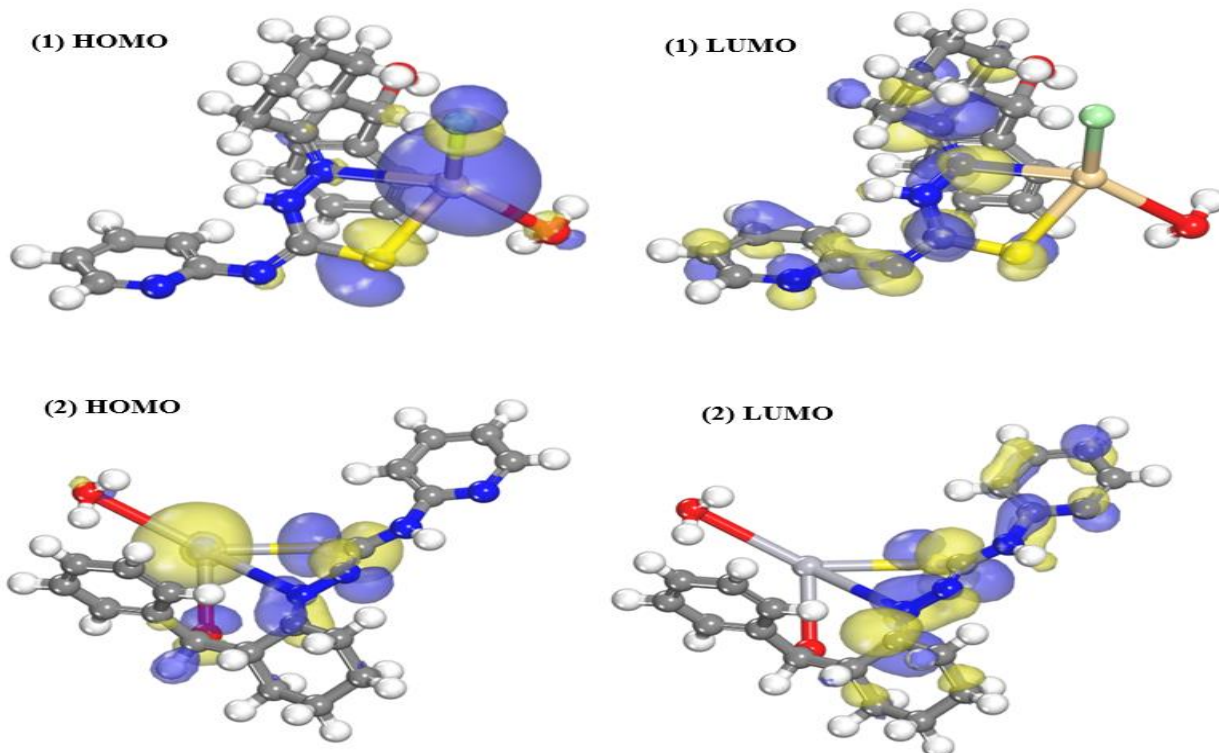


Figure 7: HOMO, LUMO Orbitals for Cd^{2+} (1), and Hg^{2+} (2) Complexes

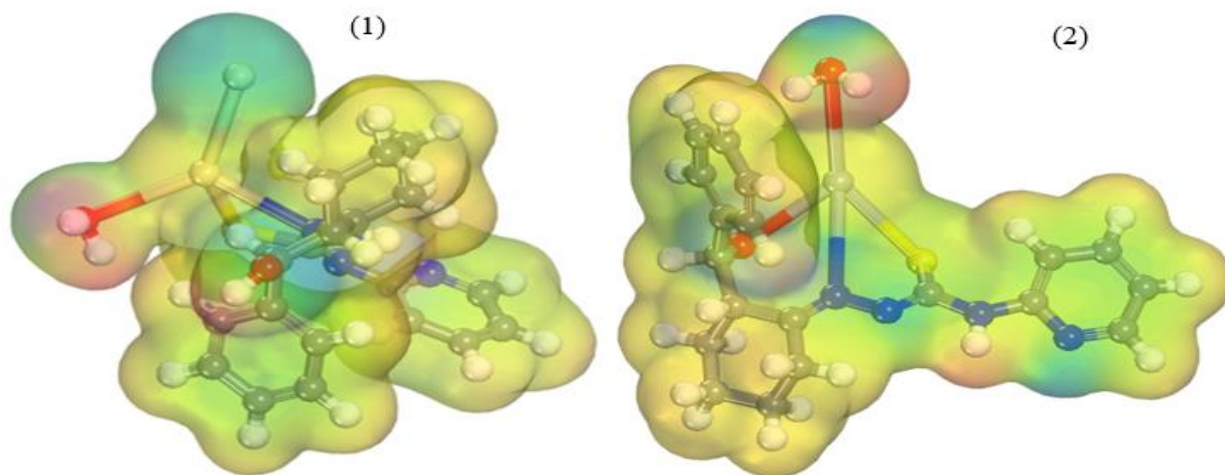


Figure 8: Cd^{2+} (1), and Hg^{2+} (2) Complexes Colored MESP Maps

3. Materials and methods

3.1. Reagents

All reagents and materials used in this work including 4(2-pyridyl) thiosemicarbazone, $\text{CdCl}_2 \cdot \text{H}_2\text{O}$, HgCl_2 , Ethyl Alcohol, and Diethyl ether were fetched from Sigma Aldrich without any further purification.

3.2. Characterization

Elemental analyses (C, H N, and S quantities) were determined utilizing Thermo-Fisher Analyzer. The amounts of Cd^{2+} , Hg^{2+} , and Cl ions were determined via gravimetric and volumetric analyses [12]. FT-IR spectral analysis was performed using KBr discs in range (4000-400 cm^{-1}) on Mattson 5000 spectrophotometer. Moreover, DTG-60 Shimadzu thermogravimetric analyzer was used for thermogravimetric analyses (TGA, DTG) with heating rate = (10 $^\circ\text{C}/\text{min}$) and N_2 atmosphere with (20 mL/min) gas flow rate. Finally, for DFT modeling, Materials Studio software was used to perform all calculations.

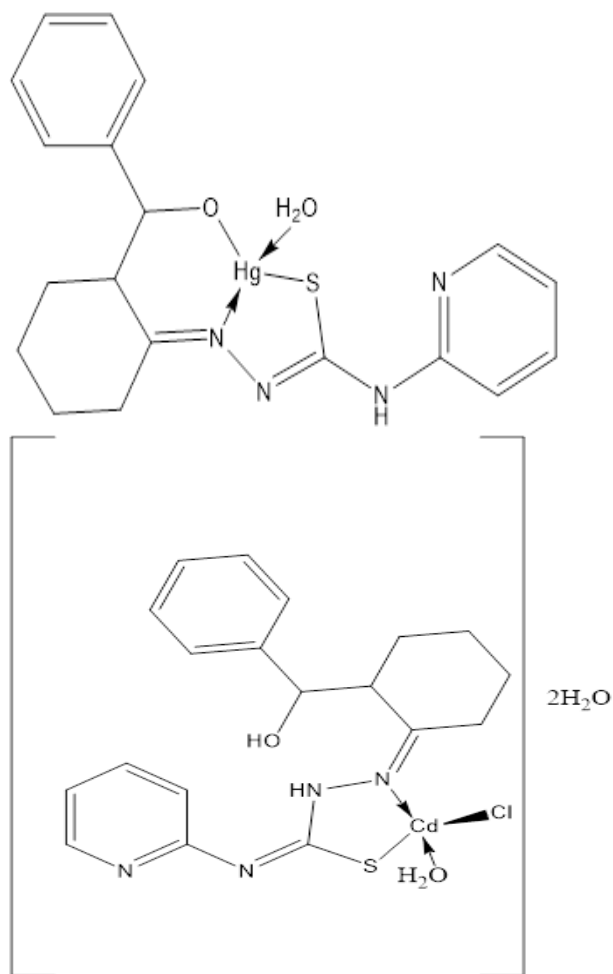


Figure 9: Cd^{2+} , and Hg^{2+} Complexes Proposed Tetrahedral Structures.

3.3. Synthesis of Complexes

1 mmol of solid ligand (E)-2-((R)-2-((R)-hydroxy(phenyl)methyl)cyclohexylidene)-N-(pyridin-2-yl)hydrazine-1-carbothioamide) was refluxed with 1 mmol of $\text{CdCl}_2 \cdot \text{H}_2\text{O}$, or HgCl_2 salt at 80 $^\circ\text{C}$ for 3 hours in presence of 15 ml absolute ethanol, the precipitate was then isolated, filtered, washed, dried, and purity confirmed using TLC. Cd^{2+} complex (1) (Figure. 9) is beige color, with 78% yield, m.p.= 180 $^\circ\text{C}$, M.F. = $\text{C}_{19}\text{H}_{27}\text{CdClN}_4\text{O}_4\text{S}$, M.W. = 555.37 g/m, found (calculated) elemental analysis C= 40.35 (41.09), H= 4.50 (4.90), N= 9.95 (10.09), S= 5.85 (6.17), and Cd= 18.50 (20.24). Hg^{2+} complex (2) (Figure 9) is orange color, with 75% yield, m.p.= 200 $^\circ\text{C}$, M.F. = $\text{C}_{19}\text{H}_{22}\text{HgN}_4\text{O}_2\text{S}$, M.W. = 571.06 g/m, C= 40.20 (39.96), H= 3.64 (3.88), N= 9.25 (9.81), S= 4.98 (5.61), and Hg= 38.00 (35.13).

Conclusion

Thiosemicarbazone metal complexes are very promising area of research regarding their ability to function as active agents in industry and medicine, in this work we prepared Cd^{2+} , and Hg^{2+} new thiosemicarbazone metal complex derived from beta hydroxy carbonyl, characterized by FT-IR spectra, and thermal analysis, also we have used Materials software to assess the complexes by DFT calculations, the complexes are proposed to have a tetrahedral structures.

4. References

- 1 M.S. Ali, F.A. El-Saied, M.M.E. Shakhofa, S. Karnik, L.A. Jaragh-Alhadad, (2023) Synthesis and characterization of thiosemicarbazone metal complexes: Crystal structure, and antiproliferation activity against breast (MCF7) and lung (A549) cancers, *Journal of Molecular Structure*, 1274 134485 DOI:<https://doi.org/10.1016/j.molstruc.2022.134485>.
- 2 T. Bal-Demirci, G. Congur, A. Erdem, S. Erdem-Kuruca, N. Özdemir, K. Akgün-Dar, (2015) B. Varol, B. Ülküseven, Iron(III) and nickel(II) complexes as potential anticancer agents: synthesis, physicochemical and structural properties, cytotoxic activity and DNA interactions, *New Journal of Chemistry*, **39** 5643-5653 DOI: <https://doi.org/10.1039/C5NJ00594A>.
- 3 H. Zhang, F. Xie, M. Cheng, F. Peng, (2019) Novel Meta-iodobenzylguanidine-Based Copper Thiosemicarbazide-1-

- guanidinomethylbenzyl Anticancer Compounds Targeting Norepinephrine Transporter in Neuroblastoma, *Journal of Medicinal Chemistry*, **62** 6985-6991 DOI: <https://doi.org/10.1021/acs.jmedchem.9b00386>.
- 4 B.N. Goswami, J.C.S. Katakya, J.N. Baruah, (1984) Synthesis and antibacterial activity of 1-(2,4-dichlorobenzoyl)-4-substituted thiosemicarbazides, 1,2,4-triazoles and their methyl derivatives, *Journal of Heterocyclic Chemistry*, **21** 1225-1229 DOI: <https://doi.org/10.1002/jhet.5570210460>.
- 5 M.S. More, P.G. Joshi, Y.K. Mishra, P.K. Khanna, (2019) Metal complexes driven from Schiff bases and semicarbazones for biomedical and allied applications: a review, *Materials Today Chemistry*, **14** 100195 DOI: <https://doi.org/10.1016/j.mtchem.2019.100195>.
- 6 A. Fetoh, M.A. Mohammed, M.M. Youssef, G.M. Abu El-Reash, (2019) Characterization, cyclic voltammetry and biological studies of divalent Co, Ni and Cu complexes of water-soluble, bioactive and photoactive thiosemicarbazone salt, *Journal of Molecular Liquids*, **287** 110958 DOI: <https://doi.org/10.1016/j.molliq.2019.110958>.
- 7 A. Fetoh, M.A. Mohammed, M.M. Youssef, G.M.A. El-Reash, (2023) Investigation (IR, UV-visible, fluorescence, X-ray diffraction and thermogravimetric) studies of Mn(II), Fe(III) and Cr(III) complexes of thiosemicarbazone derived from 4-pyridyl thiosemicarbazide and monosodium 5-sulfonatosalicylaldehyde and evaluation of their biological applications, *Journal of Molecular Structure*, **1271** 134139 DOI: <https://doi.org/10.1016/j.molstruc.2022.134139>.
- 8 Yuan, J. Hu, Y. Guo, J. Zhang, S. Zhang, K. Zhang, J.a. Zhao, H. Hou, (2021) Nuclei DNA and mitochondria dual damages induced by thiosemicarbazone tripyridyl copper complexes with potential anti-tumor activity, *Polyhedron*, **203** 115225 DOI: <https://doi.org/10.1016/j.poly.2021.115225>.
- 9 K. Turk, A.M. Grześkiewicz, C.N. Banti, S.K. Hadjikakou, M. Kubicki, I.I. Ozturk, (2022) Synthesis, characterization, and biological properties of mono-, di- and poly-nuclear bismuth(III) halide complexes containing thiophene-2-carbaldehyde thiosemicarbazones, *Journal of Inorganic Biochemistry*, **237** 111987 DOI: <https://doi.org/10.1016/j.jinorgbio.2022.111987>.
- 10 J. Padmanabhan, R. Parthasarathi, V. Subramanian, P. Chattaraj, (2007) Electrophilicity-based charge transfer descriptor, *The Journal of Physical Chemistry A*, **111** 1358-1361 DOI: <https://doi.org/10.1021/jp0649549>.
- 11 R.G. Pearson, (1989) Absolute electronegativity and hardness: applications to organic chemistry, *The Journal of Organic Chemistry*, **54** 1423-1430 DOI: <https://doi.org/10.1021/jo00267a034>.
- 12 A.I. Vogel, G.H. Jeffery, (1989). Vogel's textbook of quantitative chemical analysis, (No Title),